Nat. Hazards Earth Syst. Sci., 11, 3097–3105, 2011
www.nat-hazards-earth-syst-sci.net/11/3097/2011/
doi:10.5194/nhess-11-3097-2011

Natural Hazards and Earth System Sciences

Assessment of Arias Intensity of historical earthquakes using modified Mercalli intensities and artificial neural networks

G-A. Tselentis

University of Patras, Seismological Lab, RIO 265 04, Greece

Received: 21 May 2011 – Revised: 14 September 2011 – Accepted: 15 September 2011 – Published: 2 December 2011

Abstract. This paper presents the development of a non-parametric forecast model based on artificial neural networks for the direct assessment of Arias Intensity corresponding to a historic earthquake using seismic intensity data. The neural models allow complex and nonlinear behaviour to be tracked. Application of this methodology on earthquakes with known instrumental data from Greece, showed that the artificial neural network forecast model have excellent data synthesis capability.

1 Introduction

With widespread use of strong motion recorders, it is possible to obtain engineering seismic parameters (ESP), such as Arias Intensity (I_a) for the majority of strong earthquakes that occur today. Many investigators have compared these parameters to seismic intensity data, but have found that the correlation is usually poor and the relationships are highly nonlinear in nature (e.g., Tselentis and Vladutu, 2010).

Since most loss-estimation methodologies (seismic scenarios) in use today (Kaestli et al., 2006), are based on the distribution of ESP, the task of forecasting these parameters from seismic intensity is very important to quantify the effect of historical earthquakes for which no instrumental data are available. In the present investigation by seismic intensity, we refer to the Modified Mercalli Intensity scale (MMI).

Arias Intensity, as defined by Arias (1970), is the total energy per unit weight stored by a set of undamped simple oscillators at the end of an earthquake. The Arias Intensity for ground motion in the X (i.e., E-W) direction is calculated as follows

$$I_{aX} = \frac{2\pi}{g} \int_0^{t_0} a_X^2(t)\mathrm{d}t \quad (1)$$

where $a_X(t)$ is the corresponding acceleration time history and t_0 is the total duration of the ground motion. In the present investigation by I_a, we mean the sum of the two horizontal components $I_a = I a_{EW} + I a_{NS}$.

We attempt to use a flexible class of statistical models to investigate the relationship of parameters derived from seismic intensity to I_a, which essentially becomes a pattern-matching problem and is implemented by the use of artificial neural networks (ANN). The significant advantage of the ANN approach in estimating I_a from seismic intensity data is that one does not need to have a well-defined process for algorithmically converting an input to an output. All we need is a set of representative examples of the desired mapping then the ANN automatically adapts itself to reproduce the desired output when presented with a training sample input.

2 MMI intensity relations

There are many ESP to MMI estimation equations proposed by various researchers. A significant limitation of these equations is that most of them consider only ground motion to intensity estimation, with intensity the depended value in the regression. Thus, one should only use these equations for assessing the MMI, given a ground motion and not to assess ESP from intensity data.

Despite the doubtful conceptual validity of the MMI-ESP correlations, this approach offers the possibility of transforming quantitative, readily observed data (intensity) into parameters which are useful for engineering purposes (such as I_a) and is widely used to evaluate the historical earthquakes for which no instrumental data are available.

A key task into the development of ShakeMaps (Wald et al., 1999a) is the construction of regional specific relationships between ESP and MMI. During the last decades, many

Correspondence to: G-A. Tselentis
(tselenti@geology.upatras.gr)

attempts were made to develop region specific ESP-intensity relationships (Ambraseys, 1974; Atkinson and Kaka, 2007; Atkinson and Sonley, 2000; Cabanas et al., 1997; Kaka and Atkinson, 2004; Kaliopoulos et al., 1998; Margottini et al., 1992; Murphy and O'Brien, 1977; Panza et al., 1997; Schenk et al., 1990; Trifunac and Brady, 1975; Wald et al., 1999b; Wu et al., 2003). These studies are region specific, and the proposed ESP-intensity relationships are suitable to that particular seismotectonic and building characteristics of the regions.

Allen and Wald (2009) evaluated the performance of several modern ESP-MMI equations (Wald et al., 1999; Atkinson and Kaka, 2007; Tselentis and Danciu, 2008) and found that these relations specify a standard deviation of the order of one MMI unit. Since the successful application of Shake maps in seismic risk assessment (Wald et al., 1999a), various investigators have addressed the problem of assessing intensities from ESP. This conversion is usually necessary with historical earthquake studies, where intensity data are available and is of interest to assess ESP.

Although it is common practice to simply invert ESP-MMI relations to get an ESP, it is not necessarily correct (Wald et al., 1999a). An exception is the relationship proposed by Faenza and Michelini (2010), since it is based on an orthogonal distance regression and can be applied both ways, i.e., derive PGA from MMI and vice versa.

In Greece, Theodulidis and Papazachos (1992, 1994) and Tselentis and Danciu (2008) proposed various empirical relations between MMI and ESP. Koliopoulos et al. (1998), produced an empirical regression equation for MMI and various ground motion parameters. The main goal of the study was to investigate the relationship between duration and energy characteristics of Greek strong ground motion data. Recently, Tselentis and Vladutu (2010) followed a genetic algorithm approach to investigate the relation between MMI and various ESP.

3 Data

The database used for this study is derived primarily from readily available strong motion data that have been recorded for felt earthquakes in Greece in the last 40 yr and provided by the European Strong Motion Database (Ambraseys et al., 2004).

The horizontal components of ground motion have been selected, no vertical components were considered and it was decided to treat each horizontal component independently rather than to introduce a vector sum of the two components, because the maximum values of ground motion parameters are not realized simultaneously in each component and, therefore, any computed quantities based on summation would be the upper bounds of the parameters of interest, thus, limiting their practical use (Koliopoulos et al., 1998).

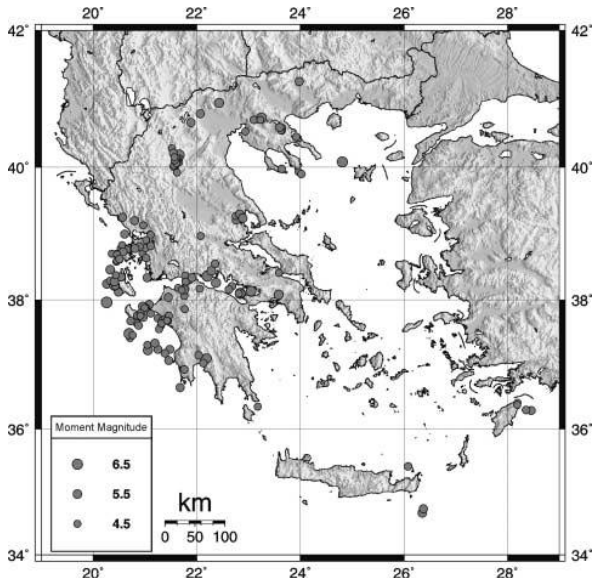

Fig. 1. Epicentral distribution of earthquakes used in the present analysis.

The final dataset consists of 328 time histories recorded from earthquakes which occurred in Greece (Fig. 1). Table 1 provides a list of these earthquakes. No correction has been applied to the selected records because these records were available in an already corrected form. The magnitude scale, which we will refer to as M in this article, corresponds to the moment magnitude (Hanks and Kanamori, 1979).

For the selected dataset based on data from Greece, M is ranging between 4.5 and 6.6.

Since most of the events are offshore and for those onshore the surface geology does not often show any evident faulting, it is impossible to use a fault distance definition like the closest distance to the fault rupture or to the surface projection of the rupture. Thus, we decided to use the epicentral distance. Hypocentral depths of the selected earthquakes are in the interval 0 to 30 km with a mean of 11.14 km. Most of the intensity information was available through the European Strong Motion Database (Ambraseys et al., 2004) and completed by the macroseismic database developed by Kalogeras et al. (2004). The macroseismic database covers most of the strong earthquakes occurred in Greece and for each event MMI values are assigned to every recording station.

The corresponding, to each earthquake, isoseisms were constructed using the kriging methodology. Kriging is a statistical technique that estimates unknown values at specific points in space using data values from known locations. The main assumption when using kriging is that the data analysed are samples of a regionalized variable, as is assumed to be the case with intensity data. A regionalized variable varies continuously in such a manner that points near each

Table 1. Database of strong motion records used. R is the epicentral distance, M_w is the body wave magnitude, Soil parameter is 0 for rock ($Vs > 800\,m\,s^{-1}$), 1 for stiff soil ($Vs = 360 - 665\,m\,s^{-1}$) and 2 for soft soil ($Vs = 200 - 360\,m\,s^{-1}$).

Earthquake Name	Date	R (km)	M_w	soil	MMI	I_a
Ionian	04/11/1973	15	5.8	0	7	0.5021
Ionian	4/11/1973	9	4.8	0	5	0.0238
Patras	29/01/1974	13	4.5	0	5	0.0006
Achaia	18/05/1978	8	4	0	5	0.0006
Volvi	20/06/1978	29	6.2	0	7	0.1737
Volvi	20/06/1978	29	6.2	0	7	0.2071
Alkion	24/02/1981	20	6.6	0	7	0.8195
Alkion	24/02/1981	19	6.6	0	8	0.8882
Alkion	25/02/1981	25	6.3	0	6	0.1826
Preveza	3/10/1981	28	5.4	1	7	0.2569
Preveza	3/10/1981	42	5.4	0	7	0.0483
Kefallinia island	17/01/1983	104	6.9	0	6	0.1058
Kefallinia island	17/01/1983	124	6.9	1	5	0.0156
Kefallinia (after	23/03/1983	11	5.2	0	5	0.0284
Kefallinia (after	23/03/1983	72	6.2	0	4	0.0118
Elis	13/08/1985	18	4.9	1	5	0.0132
Near coast of Pre	31/08/1985	13	5.2	1	6	0.0352
Near coast of Pre	31/08/1985	21	5.2	0	6	0.0389
Kalamata	13/09/1986	11	5.9	1	8	0.7413
Kalamata (aftersh	15/09/1986	3	4.9	1	7	0.2818
Dodecanese	10/5/1987	26	5.3	1	5	0.0179
Ionian	24/04/1988	13	4.8	0	6	0.2044
Etolia	18/05/1988	23	5.3	2	7	0.1454
Kyllini	16/10/1988	36	5.9	1	7	0.1416
Kyllini	16/10/1988	14	5.9	1	7	0.2949
Patras	22/12/1988	5	4.9	1	6	0.0307
Patras	22/12/1988	14	4.9	0	6	0.0056
Patras	31/08/1989	21	4.8	0	5	0.0185
Aigion	17/05/1990	20	5.30	1	6	0.0284
Plati	8/8/1990	36	5.10	1	4	0.0033
Mataranga	30/05/1992	28	5.2	1	4	0.005
Mataranga	30/05/1992	34	5.2	0	3	0.0093
Tithorea	18/11/1992	25	5.9	1	5	0.0129
Gulf of Corinth	2/4/1993	9	5.30	0	6	0.0535
Near coast of Fil	34092	27	5.2	1	5	0.0046
Kallithea	18/03/1993	41	5.8	0	4	0.0057
Pyrgos (foreshock	26/03/1993	16	4.9	1	5	0.0054
Pyrgos (foreshock	26/03/1993	10	4.9	1	5	0.0091
Pyrgos	26/03/1993	10	5.4	0	7	0.3325
Pyrgos	26/03/1993	24	5.4	1	6	0.0631
Mouzakaiika	13/06/1993	48	5.3	0	5	0.0657
Patras	14/07/1993	30	5.6	1	5	0.0196
Patras	14/07/1993	54	5.6	1	5	0.0037
Patras	14/07/1993	37	5.6	0	5	0.0096
Patras	14/07/1993	27	5.6	1	6	0.0214
Patras	14/07/1993	10	5.6	0	7	0.1789
Gulf of Corinth	4/11/1993	18	5.3	1	4	0.004
Gulf of Corinth	4/11/1993	10	5.3	1	5	0.0449
Komilion	25/02/1994	16	5.4	0	7	0.201
Komilion	25/02/1994	29	5.4	1	6	0.0231
Ionian	27/02/1994	27	4.8	0	5	0.0176
Ano Liosia	36350	20	6	0	7	0.1537
Ano Liosia	9/7/1999	16	6	1	7	0.3382
Ano Liosia	9/7/1999	17	6	0	7	0.0952
Ano Liosia	36350	19	6	1	7	0.0902
Ano Liosia	9/7/1999	19	6	1	6	0.0434
Ano Liosia	9/7/1999	20	6	1	6	0.0522
Ano Liosia	9/7/1999	18	6	1	6	0.064
Ano Liosia	9/7/1999	14	6	1	7	0.2942
Ano Liosia	9/7/1999	14	6	1	7	0.5939

Table 1. Continued.

Earthquake Name	Date	R (km)	M_w	soil	MMI	I_a
Astakos	22/01/1988	27	5.1	2	5	0.0016
Agrinio	8/3/1988	6	4.9	2	6	0.0136
Etolia	18/05/1988	20	5.3	1	6	0.0166
Etolia	22/05/1988	21	5.4	1	5	0.0123
Kefallinia island	23/06/1992	16	5	1	7	0.1409
Skydra-Edessa	18/02/1986	2	5.3	1	6	0.0601
Griva	21/12/1990	36	6.1	1	7	0.129
Griva	21/12/1990	37	6.1	1	6	0.0187
Gulf of Corinth	32206	19	4.5	1	5	0.0065
Gulf of Corinth	3/4/1988	19	4.5	1	5	0.0093
Gulf of Corinth	7/5/1988	19	4.9	1	5	0.018
Tithorea	18/11/1992	61	5.9	1	5	0.0096
Kranidia	25/10/1984	23	5.5	2	6	0.0048
Near coast of Fil	5/3/1993	54	5.2	2	5	0.0079
Gulf of Kiparissi	7/9/1985	37	5.4	2	5	0.0045
Kalamata (aftersh	6/10/1987	17	5.3	2	6	0.0161
Peratia	22/05/1986	7	4.1	0	3	0.0015
Near NW coast of	27/02/1987	52	5.7	0	5	0.0124
Levkas island	11/10/1992	5	4.6	0	5	0.0105
Mouzakaiika	13/06/1993	48	5.3	0	5	0.018
Komilion	25/02/1994	15	5.4	0	7	0.1405
Ionian	27/02/1994	26	4.8	0	5	0.0158
Ierissos	26/08/1983	15	5.1	2	6	0.0643
Paliouri	4/10/1994	5	5.1	1	5	0.0089
Patras	15/05/1989	6	4.8	1	5	0.0078
Patras	31/08/1989	21	4.8	1	5	0.0237
Mataranga	30/05/1992	34	5.2	1	5	0.0142
Patras	14/07/1993	10	5.6	1	7	0.1589
Patras (aftershoc	14/07/1993	11	4.6	1	4	0.0021
Mataranga	30/05/1992	33	5.2	1	5	0.0137
Patras	14/07/1993	9	5.6	1	7	0.1601
Kyllini	16/10/1988	78	5.9	1	4	0.0034
Patras	22/12/1988	14	4.9	1	6	0.0049
Kyllini	16/10/1988	49	5.9	0	6	0.0116
Trilofon	20/10/1988	7	4.8	0	5	0.0007
Komilion	25/02/1994	12	5.4	1	6	0.0676
Kyllini (foreshoc	22/09/1988	23	5.3	1	5	0.0133
Almiros (aftersho	16/07/1980	3	5	1	6	0.0611
Almiros (aftersho	8/11/1980	14	5.2	1	6	0.037
Almiros (aftersho	26/09/1980	10	4.8	1	5	0.021
Kefallinia (after	23/03/1983	9	6.2	1	6	0.3968
Drama	11/9/1985	19	5.2	1	6	0.0193
Drama	11/9/1985	51	5.2	2	5	0.0208
Kalamata (aftersh	15/09/1986	12	4.9	1	6	0.0187
Kremidia (aftersh	25/10/1984	16	5	2	6	0.2228
Ierissos	26/08/1983	42	5.1	2	5	0.0326
Near coast of Pre	31/08/1985	13	5.2	1	6	0.0258
Kefallinia (after	23/03/1983	65	6.2	1	5	0.0173
Near SE coast of	10/4/1984	17	5	1	5	0.0143
Kyllini	16/10/1988	16	5.9	1	5	0.0053
Kyllini (aftersho	23/10/1988	10	4.3	1	5	0.0038
Kyllini (aftersho	31/10/1988	14	4.8	1	5	0.0117
Kyllini (aftersho	27/11/1988	14	4.5	1	4	0.0083
Kyllini (aftersho	22/10/1988	12	4.5	1	5	0.0041
Kyllini (aftersho	23/10/1988	7	4.4	1	5	0.0078
Kyllini (aftersho	27/11/1988	19	4.5	0	4	0.0063
Kyllini (aftersho	20/10/1988	16	4.2	0	5	0.0067
Kyllini (aftersho	22/10/1988	16	4.5	0	5	0.0109
Volvi	20/06/1978	78	6.2	0	5	0.0054
Kalamata	13/10/1997	48	6.4	2	7	0.1921
Strofades	18/11/1997	90	6.6	2	6	0.0605
Pyrgos	8/11/1996	2	4.7	0	6	0.0259
Levkas island	23/04/1996	6	3.9	1	5	0.0034

Table 1. Continued.

Earthquake Name	Date	R (km)	M_w	soil	MMI	I_a
Off coast of Magi	30475	76	6.6	2	6	0.0264
Kefallinia island	23/01/1992	14	5.6	1	7	0.1562
Kozani (aftershoc	14/05/1995	6	4.5	1	6	0.0214
Kozani (aftershoc	15/05/1995	9	5.2	1	7	0.136
Kozani (aftershoc	17/05/1995	16	5.3	1	6	0.0712
Kozani	13/05/1995	77	6.5	1	6	0.0182
Kozani	13/05/1995	71	6.5	2	4	0.0115
Arnaia	4/05/1995	32	5.3	1	5	0.0075
Kozani (aftershoc	19/05/1995	16	5.2	1	6	0.3339
Kozani (aftershoc	6/11/1995	3	4.8	1	6	0.0677
Kozani	13/05/1995	93	6.5	1	4	0.0181
Kozani	13/05/1995	72	6.5	1	6	0.0172

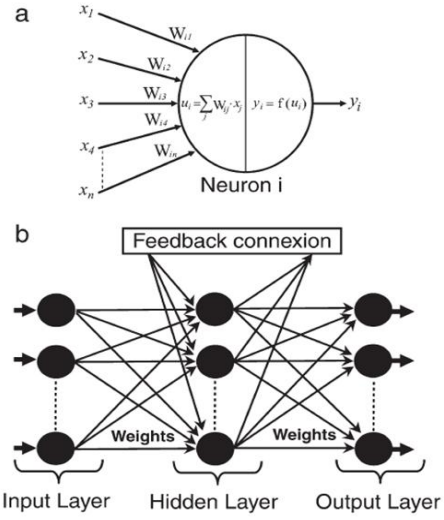

Fig. 2. General topology of a feed-forward ANN with one hidden layer.

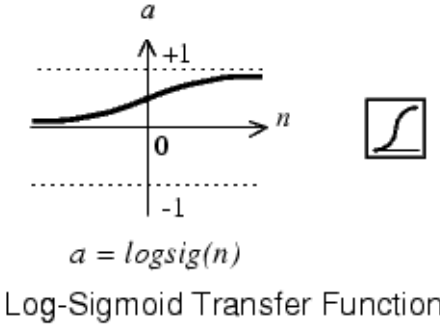

Fig. 3. The nonlinear S-shaped sigmoid activation function used in the present investigation.

other, have a certain degree of spatial correlation, but points that are widely separated are statistically independent.

The kriging estimator applied in the macroseismic dataset considered in the present paper is given by

$$I_j = \sum_{i=1}^{n} w_{ij} \mathrm{MMI}_j \tag{2}$$

Where I_j is the predicted intensity value at any grid node, n is the number of points used to interpolate at each node, MMI_i is the intensity value at the i-th point and w_{ij} is the weight associated with the i-th data value when estimating I_j. The weights are solutions of a system of linear equations which are obtained by assuming that I is a sample-path of a random process and that the error of prediction is minimal.

The kriging algorithm assigns weights to each point based on the distance between the point to be interpolated and the data location (h), as well as the inter-data spacing. Other parameters, such as length scale, repeatability and direction dependence of data are also considered for assigning weights. These parameters are entred into the algorithm via the variogram $\gamma(h)$, which is an analytical tool that quantifies the degree of spatial autocorrelation of data.

In the present investigation, the isoseismals, that more accurately represented the observed intensity data field, were chosen by modelling a simple linear variogram based on the kriging options of Surfer Package from Golden Software. A detailed explanation of the kriging algorithm and the variogram parameters can be found in De Rubeis et al. (2005).

4 Artificial neural network

An artificial neural network is an information processing paradigm that is inspired by the way biological nervous systems, such as the brain, process information. The most basic element of the human brain is a specific type of cell, which provides us with the ability to remember, think and apply previous experiences to our every action. These cells are known as neurons. The power of the brain comes from the number of neurons and the multiple connections (synapses) between them.

Table 2. Network performance for a different number of neurons in the hidden layer. AIC refers to the Akaike's Information Criterion defined by AIC $= T\ln(\mathrm{RSS})+2k$, where k is the number of regressors, T the number of observations and RSS the residual sum of square.

ANN	Weights	Train Error	Validation Error	AIC	Correlation	R-Squared
[6-1-1]	9	0.023	0.055554	−407.1	0.831	0.659
[6-15-1]	121	0.026	0.051017	−471.4	0.817	0.663
[6-9-1]	73	0.024	0.049607	−575.9	0.82	0.663
[6-5-1]	41	0.022	0.057709	−645.3	0.84	0.708
[6-12-1]	97	0.028	0.050409	−512.0	0.806	0.511
[6-7-1]	57	0.028	0.05679	−592.0	0.811	0.615
[6-10-1]	81	0.025	0.051625	−556.3	0.807	0.613
[6-8-1]	65	0.0191	0.053817	−608.7	0.913	0.833

Figure 2 shows a simplified view of a ANN. It consists of a network of simple processing elements (artificial neurons) which are organised in several layers: an input layer (which has the number of neurons linked to the dimensionality of the input), one or several hidden layers and an output layer. The hidden layer provides a representation for the inputs.

When one presents, at the network, a form to be learned, the neurons simultaneously start a state of activity which causes a small modification of the synaptic between the forces. It follows a quantitative reconfiguration of the whole of the synapses, some of them become very strong, the others become weak. The learned form is not directly memorized at a precise place; it corresponds in a particular energy state of the network, a particular configuration of the activity of each neuron, in a very large case of possible configurations. This configuration is supported by the values of the synaptic forces (Haykin, 1999).

Let Y_j^s represents the output of the j-th neuron at layer s, W_{ij}^s is the weight connecting the i-th neuron in layer s to the j-th neuron at layer $s-1$. The neurons have their activation function characterised by a nonlinear function (like the Sigmoid function in Fig. 3). This function maps the output to its input and can be expressed by the following equation

$$Y_j^s = f(b_+ \sum_{i=1}^{R} W_{ji}^s \times Y_i^{s-1}) \tag{3}$$

where b is the bias.

This relation allows, by knowing the input of the first layer of the network, to gradually calculate the value of the global output of the network, thus, ensuring the forward propagation. When one compares this output with the desired output, one can calculate the error function, generally given by

$$e = \frac{1}{2}\left(Y - \bar{Y}\right)^2 \tag{4}$$

where Y is the desired output and $\left(\bar{Y}\right)$ the obtained output. The direction in which the weights are updated is given by the negative of the gradient of **e** with respect to every element of the weight. This process consists in minimizing **e** by a gradient descent. Thus, we try to modify the synaptic

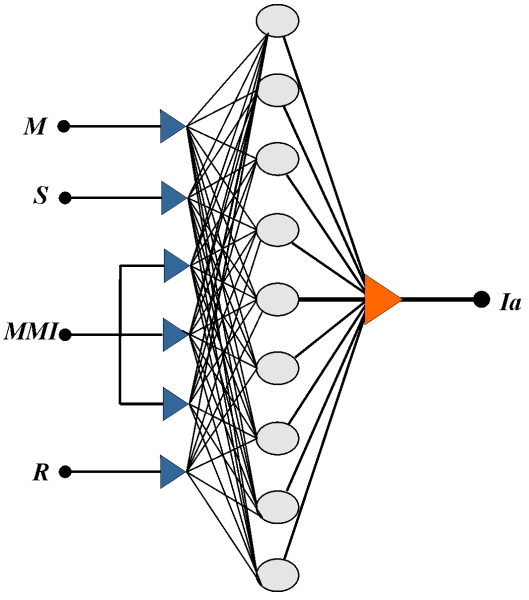

Fig. 4. Topology of the feed-forward k-NN-type ANN used in the present study. Input parameters are magnitude M_w, Soil parameter S, MMI and epicentral distance R.

weights in order to reduce **e**. This is carried out using the following relation

$$\Delta w_{ij}^s = -\mu(e_j^s Y_i^{s-1})_n + (\Delta w_{ji}^s)_{n-1} \tag{5}$$

where μ is the learning rate parameter and usually takes values between 0 and 0.5. The quantity e_j^s is the local error of the j-th neuron in the s layer. Weights and bias terms are first initialized to random values. In general, there are no strict rules to determine the network configuration for optimum training and prediction.

5 ANN model for seismic intensity

Data from earthquakes and locations for which both MMI data and Greek strong motion records are available (Table 1) was used to build and train an ANN. Earthquake magnitude,

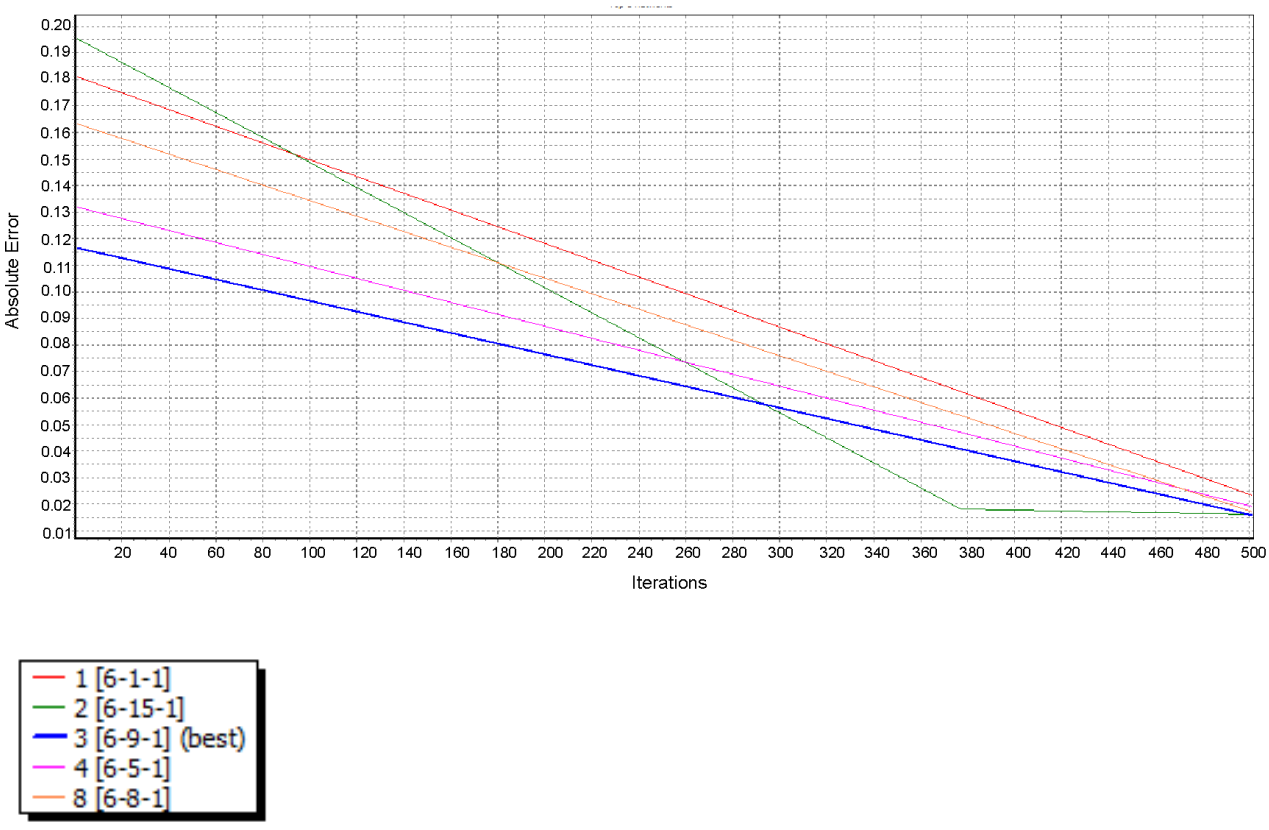

Fig. 5. Absolute ANN error versus No of iterations for different number of neurons in the hidden layer.

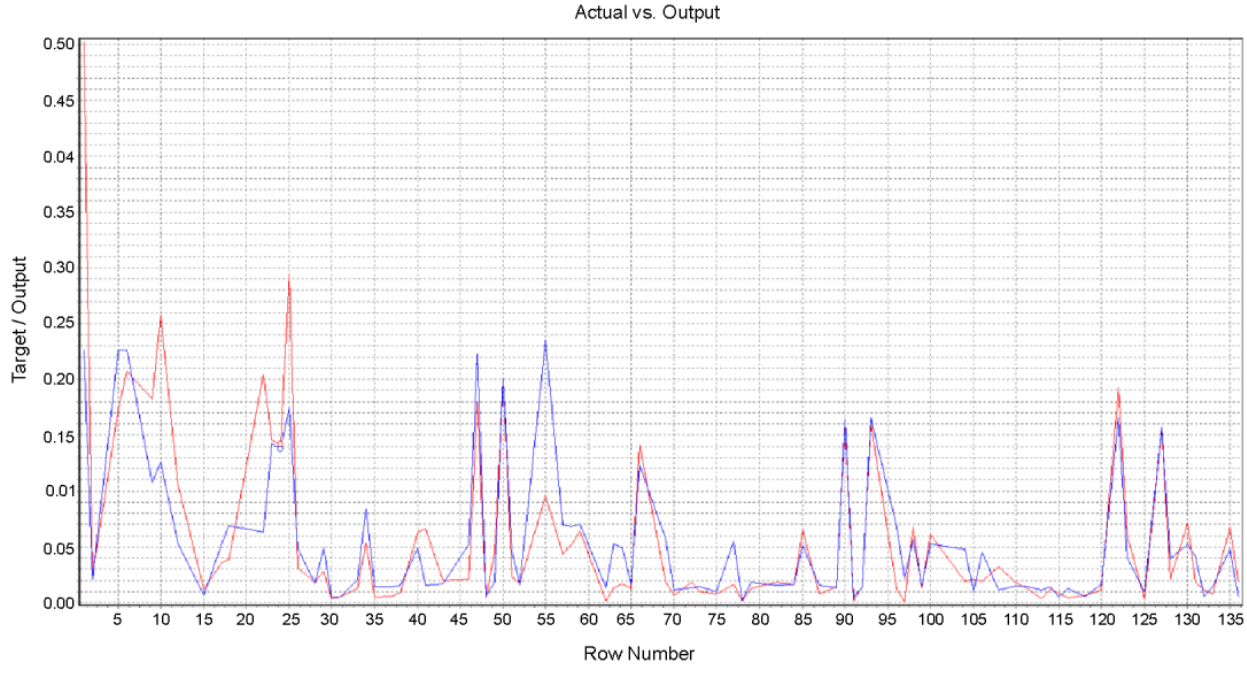

Fig. 6. Comparison of real (red line) and predicted values.

soil conditions (rock, soil, soft soil), epicentral distance and MMI values were used as input layer variables to a multilayered feed forward ANN. The single output layer variable was the I_a value.

After trying various numbers of hidden layers, we found that the best type of network for the present investigation is that consisting of one hidden layer resulting in a total of three layers (Fig. 4). The Sigmoid function (Fig. 3), was used for the transfer function of the hidden neurons. We changed the number of neurons in the hidden layers and those that gave the smallest error are depicted in Table 2. The performance of the ANN was found to deteriorate as the number of hidden neurons increased farther than the number 15.

For supervised training of the ANN, a subset of two thirds of the total records was used. The individual sites assigned to this training set were selected at random from the complete set of records. The other third of the data was used for testing the ANN after it had been trained.

Figure 5 depicts the ANN absolute error, for various numbers of neurons in the hidden layer, versus the training epoch (iterations). Judging from this figure, we see that the ANN with 9 neurons in the hidden layer has the lowest error and is selected for further data processing.

Finally, a comparison between the results predicted by the ANN and the test data are presented in Fig. 6. The correlation between the predicted and real data is excellent considering the strong nonlinear character of the relation between MMI and I_a.

6 Conclusions

In the present investigation, we examined the relation between MMI and I_a using a database consisting of Greek earthquakes and employing ANN. It is shown that an ANN can be used to predict I_a from MMI data despite the strong nonlinear nature of the problem. This result is of particular importance in studying historical earthquakes for which there is a big database in Greece.

Acknowledgements. I want to thank M. E. Contadakis for editing the current manuscript and L. Danciu for compiling the Macroseismic data.

Edited by: M. E. Contadakis
Reviewed by: two anonymous referees

References

Allen, T. I. and Wald, D. J.: Evaluation of ground-motion modelling techniques for use in Global ShakeMap: a critique of instrumental ground-motion prediction equations, peak ground motion to macroseismic intensity conversions, and macroseismic intensity predictions in different tectonic settings, US Geological Survey Open-File Report 2009-1047, Golden, USA, 114 pp., 2009.

Ambraseys, N. N.: The correlation of intensity with ground motions, Advancements in Engineering Seismology in Europe, Trieste, Italy, 12-23, 1974.

Ambraseys, N. N., Smit, P., Douglas, J., Margaris, B., Sigbjörnsson, R., Ólafsson, S., Suhadolc, P., and Costa, G.: Internet site for European strong-motion data, Bull. Geof. Teor. Appl., 45, 113–129, 2004.

Arias, A.: A measure of earthquake intensity, in: Seismic Design for Nuclear Power Plants, edited by: Hansen, R. J., MIT Press, Cambridge, Massachusetts, 438–483, 1970.

Atkinson, G. M. and Sonley, E.: Empirical Relationships between Modified Mercalli Intensity and Response Spectra, Bull. Seismol. Soc. Am., 90, 537–544, 2000.

Atkinson, G. M. and Kaka, S. I.: Relationships between Felt Intensity and Instrumental Ground Motion in the Central United States and California, Bull. Seismol. Soc. Am., 97, 497–510, 2007.

Cabanas, L., Benito, B., and Herraiz, M.: An approach to the measurement of the potential structural damage of earthquake ground motions, Earthq. Eng. Struct. Dyn., 26, 79–92, 1997.

De Rubeis,V., Tosi, P., Gasparini, C., and Solipaca, A.:Application of Kriging Technique to Seismic Intensity Data, Bull. Seismol. Soc. Am., 95, 540–548, 2005.

Faenza, L. and Michelini, A.: Regression analysis of MCS intensity and ground motion parameters in Italy and its application in ShakeMap, Geophys. J. Int., 180, 1138–1152, 2010.

Hanks, T. C. and Kanamori, H.: A Moment Magnitude Scale, J. Geophys. Res., 84, 2348–2350, 1979.

Haykin, S.: Neural Networks, MacMillan College Publishing Company, 2nd Edn., 1999.

Kaestli, P. and Faeh, D.: Rapid estimation of macroseismic effects and ShakeMaps using macroseismic data, 1st European Conference on Earthquake Engineering and Seismology, Geneva, Switzerland, 3–8 September 2006, Paper n. 1353, 2006.

Kaka, S. I. and Atkinson, G. M.: Relationships between Instrumental Ground-Motion Parameters and Modified Mercalli Intensity in Eastern North America, Bull. Seismol. Soc. Am., 94, 1728–1736, 2004.

Kalogeras, I. S., Marketos, G., and Theodoridis, Y.: A tool for collecting, querying and mining macroseismic data, Bull. Geol. Soc. Greece, 36, 1406–1411, 2004.

Koliopoulos, P. K., Margaris, B. N., and Klimis, N. S.: Duration and energy characteristics of Greek strong motion records, J. Earthqu. Eng., 2, 391–417, 1998.

Margottini, C., Molin, D., and Serva, L.: Intensity versus ground motion: A new approach using Italian data, Eng. Geol., 33, 45–58, 1992.

Murphy, J. R. and O'Brien, L. J.: The correlation of peak ground acceleration amplitude with seismic intensity and other physical parameters, Bull. Seismol. Soc. Am., 67, 877–915, 1977.

Panza, G. F., Cazzaro, R., and Vacari, F.: Correlation between macroseismic intensities and seismic ground motion parameters, Ann. Geofis., XL, 1371–1382, 1997.

Schenk, V., Mantlík, F., Zhizhin, M. N., and Tumarkin, A. G.: Relation between macroseismic intensity and instrumental parameters of strong motions – A statistical approach, Nat. Hazards, 3, 111–124, 1990.

Sørensen, M. B., Stromeyer, D., and Grünthal, G.: Deliverable 4.1: Generation of area-specific relationships between ground motion parameters (PGA, PGV) at certain sites, magnitude M and distance R to the causative fault and site intensities in terms of EMS-98, Databank of intensity data points and related parameters, Seismic eArly warning For EuRope, GFZ Potsdam, 19–32, 2007.

Theodulidis, N. P. and Papazachos, B. C.: Dependence of strong ground motion on magnitude-distance, site geology and macroseismic intensity for shallow earthquakes in Greece: I, Peak horizontal acceleration, velocity and displacement, Soil Dym. Earthq. Eng., 11, 387–402, 1992.

Theodulidis, N. P. and Papazachos, B. C.: Dependence of strong ground motion on magnitude-distance, site geology and macroseismic intensity for shallow earthquakes in Greece: II, horizontal pseudovelocity, Soil Dynam. Earthq. Eng., 13, 317–343, 1994.

Trifunac, M. D. and Brady, A. G.: On the correlation of seismic intensity scales with the peaks of recorded strong ground motion, Bull. Seismol. Soc. Am., 65, 139–162, 1975.

Tselentis, G. A. and Danciu, L.: Empirical Relationships between Modified Mercalli Intensity and Engineering Ground-Motion Parameters in Greece, Bull. Seismol. Soc. Am., 98, 1863–1875, 2008.

Tselentis, G-A. and Vladutu, L.: An attempt to model the relationship between MMI attenuation and engineering ground-motion parameters using artificial neural networks and genetic algorithms, Nat. Hazards Earth Syst. Sci., 10, 2527–2537, doi:10.5194/nhess-10-2527-2010, 2010.

Wald, D. J., Quitoriano, V., Heaton, T. H., and Kanamori, H.: Relationships between Peak Ground Acceleration, Peak Ground Velocity, and Modified Mercalli Intensity in California, Earthq. Spectra, 15, 557–564, 1999a.

Wald, D. J., Quitoriano, V., Heaton, T. H., Kanamori, H., Scrivner, C. W., and Worden, C. B.: TriNet "ShakeMaps": Rapid Generation of Peak Ground Motion and Intensity Maps for Earthquakes in Southern California, Earthq. Spectra, 15, 537–555, 1999b.

Wu, Y.-M., Teng, T.-l., Shin, T.-C., and Hsiao, N.-C.: Relationship between Peak Ground Acceleration, Peak Ground Velocity, and Intensity in Taiwan, Bull. Seism. Soc. Am., 93, 386–396, 2003.